On nonlinearly-induced noise in single-channel optical links with digital backpropagation

Lotfollah Beygi,[1] Naga V. Irukulapati,[1*] Erik Agrell,[1] Pontus Johannisson,[2] Magnus Karlsson,[2] Henk Wymeersch,[1] Paolo Serena,[3] and Alberto Bononi[3]

[1]*Dept. of Signals and Systems, Chalmers University of Technology, Gothenburg, Sweden.*
[2]*Dept. of Microtechnology and Nanoscience, Chalmers University of Technology, Sweden.*
[3]*Dipartimento di Ingegneria dell'Informazione, Università degli Studi di Parma, Parma, Italy.*

[*]*vnaga@chalmers.se*

Abstract: In this paper, we investigate the performance limits of electronic chromatic dispersion compensation (EDC) and digital backpropagation (DBP) for a single-channel non-dispersion-managed fiber-optical link. A known analytical method to derive the performance of the system with EDC is extended to derive a first-order approximation for the performance of the system with DBP. In contrast to the *cubic growth* of the variance of the nonlinear noise-like interference, often called nonlinear noise, with input power for EDC, a *quadratic growth* is observed with DBP using this approximation. Finally, we provide numerical results to verify the accuracy of the proposed approach and compare it with existing analytical models.

OCIS codes: (060.1660) Coherent communications; (060.2330) Fiber optics communications.

References and links

1. D. J. Costello, Jr. and G. D. Forney, Jr., "Channel coding: The road to channel capacity," *Proc. IEEE*, **95**(6), 1150–1177 (2007).
2. R.-J. Essiambre, G. Kramer, P. J. Winzer, G. J. Foschini, and B. Goebel, "Capacity limits of optical fiber networks," *J. Lightw. Technol.*, **28**(4), 662–701 (2010).
3. A. D. Ellis, J. Zhao, and D. Cotter, "Approaching the non-linear Shannon limit," *J. Lightw. Technol.*, **28**(4), 423–433 (2010).
4. E. Agrell and M. Karlsson, "Power-efficient modulation formats in coherent transmission systems," *J. Lightw. Technol.*, **27**(22), 5115–5126 (2009).
5. A. Mecozzi, "Probability density functions of the nonlinear phase noise," *Opt. Lett.*, **29**(7), 673–675 (2004).
6. K. S. Turitsyn, S. A. Derevyanko, I. V. Yurkevich, and S. K. Turitsyn, "Information capacity of optical fiber channels with zero average dispersion," *Phys. Rev. Lett.*, **91**(20), 203901 (2003).
7. M. I. Yousefi and F. R. Kschischang, "On the per-sample capacity of nondispersive optical fibers," *IEEE Trans. Inf. Theory*, **57**(11), 7522–7541 (2011).
8. K.-P. Ho, *Phase-Modulated Optical Communication Systems* (Springer, 2005).
9. L. Beygi, E. Agrell, M. Karlsson, and P. Johannisson, "Signal statistics in fiber-optical channels with polarization multiplexing and self-phase modulation," *J. Lightw. Technol.*, **29**(16), 2379–2386 (2011).
10. A. P. T. Lau, T. S. R. Shen, W. Shieh, and K.-P. Ho, "Equalization-enhanced phase noise for 100Gb/s transmission and beyond with coherent detection," *Opt. Express*, **18**(16), 17 239–17 251 (2010).
11. K.-P. Ho, A. P. T. Lau, and W. Shieh, "Equalization-enhanced phase noise induced timing jitter," *Opt. Lett.*, **36**(4), 585–587 (2011).
12. B. Goebel, R.-J. Essiambre, G. Kramer, P. J. Winzer, and N. Hanik, "Calculation of mutual information for partially coherent Gaussian channels with applications to fiber optics," *IEEE Trans. Inf. Theory*, **57**(9), 5720–5736 (2011).

#191784 - $15.00 USD Received 5 Jun 2013; revised 6 Sep 2013; accepted 20 Sep 2013; published 28 Oct 2013

13. A. T. Lau, S. Rabbani, and J. M. Kahn, "On the statistics of intrachannel four-wave mixing in phase-modulated optical communication systems," *J. Lightw. Technol.*, **26**(14), 2128–2135 (2008).
14. K.-P. Ho and H.-C. Wang, "Comparison of nonlinear phase noise and intrachannel four-wave mixing for RZ-DPSK signals in dispersive transmission systems," *IEEE Photon. Technol. Lett.*, **17**(7), 1426–1428 (2005).
15. P. Poggiolini, "The GN model of non-linear propagation in uncompensated coherent optical systems," *J. Lightw. Technol.*, **30**(24), 3857–3879 (2012).
16. H. Song and M. Brandt-Pearce, "A 2-D discrete-time model of physical impairments in wavelength-division multiplexing systems," *J. Lightw. Technol.*, **30**(5), 713–726 (2012).
17. A. Mecozzi and R.-J. Essiambre, "Nonlinear Shannon limit in pseudolinear coherent systems," *J. Lightw. Technol.*, **30**(12), 2011–2024 (2012).
18. A. Bononi, P. Serena, N. Rossi, E. Grellier, and F. Vacondio, "Modeling nonlinearity in coherent transmissions with dominant intrachannel-Four-Wave-Mixing," *Opt. Express*, **20**(7), 7777–7791 (2012).
19. P. Johannisson and M. Karlsson, "Perturbation analysis of nonlinear propagation in a strongly dispersive optical communication system," *J. Lightw. Technol.*, **31**(8), 1273–1282 (2013).
20. A. Bononi and P. Serena, "An alternative derivation of Johannisson's regular perturbation model," 2012. [Online]. Available: http://arXiv:1207.4729
21. L. Beygi, E. Agrell, P. Johannisson, M. Karlsson, and H. Wymeersch, "A discrete-time model for uncompensated single-channel fiber-optical links," *IEEE Trans. Commun.*, **60**(11), 3440–3450 (2012).
22. E. Torrengo, R. Cigliutti, G. Bosco, A. Carena, V. Curri, P. Poggiolini, A. Nespola, D. Zeolla, and F. Forghieri, "Experimental validation of an analytical model for nonlinear propagation in uncompensated optical links," *Opt. Express*, **19**(26), B790–B798 (2011).
23. G. Bosco, R. Cigliutti, A. Nespola, A. Carena, V. Curri, F. Forghieri, Y. Yamamoto, T. Sasaki, Y. Jiang, and P. Poggiolini, "Experimental investigation of nonlinear interference accumulation in uncompensated links," *IEEE Photon. Technol. Lett.*, **24**(14), 1230–1232 (2012).
24. T. Tanimura, M. Nölle, J. K. Fischer, and C. Schubert, "Analytical results on back propagation nonlinear compensator with coherent detection," *Opt. Express*, **20**(27), pp. 28 779–28 785 (2012).
25. G. P. Agrawal, *Nonlinear fiber optics*, 4th ed. (Academic Press, 2007).
26. ——, *Fiber-Optic Communication Systems*, 2nd ed. (Wiley, 2002).
27. E. Ip and J. M. Kahn, "Compensation of dispersion and nonlinear impairments using digital Backpropagation," *J. Lightw. Technol.*, **26**(20), 3416–3425 (2008).
28. F. Vacondio, O. Rival, C. Simonneau, E. Grellier, A. Bononi, L. Lorcy, J.-C. Antona, and S. Bigo, "On nonlinear distortions of highly dispersive optical coherent systems," *Opt. Express*, **20**(2), 1022–1032 (2012).
29. L. Beygi, E. Agrell, P. Johannisson, M. Karlsson, and H. Wymeersch, "The Limits of Digital Backpropagation in Nonlinear Coherent Fiber-Optical Links," *in Proceedings of European Conference and Exhibition on Optical Communication*, Amsterdam, The Netherlands, September 2012, P4.14.
30. J. G. Proakis and M. Salehi, *Digital Communications*, 5th ed. (McGraw-Hill, 2008).
31. E. Ip, "Nonlinear compensation using backpropagation for polarization-multiplexed transmission," *J. Lightw. Technol.*, **28**(6), 939 –951 (2010).
32. A. Bononi, N. Rossi, and P. Serena, "Transmission limitations due to fiber nonlinearity," *in Proc. Optic. Fiber Commun. Conf.*, p. OWO7, Mar. 2011.
33. E. Grellier and A. Bononi, "Quality parameter for coherent transmissions with Gaussian-distributed nonlinear noise," *Opt. Express*, **19**(13), 12 781–12 788 (2011).

1. Introduction

Optical networks with heterogeneous structure demand accurate channel models and performance prediction techniques to accommodate for the dynamic and static variations of the signal quality. Moreover, the Shannon channel capacity, which is used as a criterion in the design of coded modulation schemes, also requires an exact channel model and noise statistics of fiber-optical channels [1–4]. In optical fibers, the nonlinear Schrödinger equation (NLSE) describes the propagation of light. This model is nonlinear, and due to the lack of analytical solutions and the complexity of numerical approaches, deriving the statistics of such channels is in general cumbersome. Hence, many efforts have been devoted to computing the statistics for simplified models, e.g., memory-less nonlinear channels with single-polarization [5–8] and polarization-multiplexed (PM) [9] signals, partially coherent linear channels [10–12], and channels with intra-channel four-wave mixing [13, 14].

The recent progress in channel modeling of non-dispersion-managed (non-DM) fiber-optical links has provided an accurate description for the interaction of the linear chromatic dispersion

#191784 - $15.00 USD Received 5 Jun 2013; revised 6 Sep 2013; accepted 20 Sep 2013; published 28 Oct 2013

and the nonlinear Kerr effect during propagation. The key idea behind the analytical methods is to model the nonlinearly-induced noise-like interference, the so-called nonlinear noise [15], caused by the nonlinear Kerr effect as an additive white Gaussian noise (AWGN) with zero mean. The variance of this noise as a function of the power spectral density of the transmitted signal and the channel parameters can be computed using the first-order regular perturbation (RP1) provided that the nonlinearity is weak, referred to as the pseudolinear regime [2].

Two time domain models were introduced in [16, 17] using RP1 for both dispersion-managed (DM) and non-DM single polarization fiber-optical links with wavelength-division-multiplexing (WDM). These models require numerical integration and no simple closed-form were provided for the variance of nonlinear noise. A closed-form expression for the variance of nonlinear noise was introduced in [18] with a PM signal consisting of delta-like pulses using RP1 for both DM and non-DM links. The power spectral density of the nonlinear noise was studied in [15, 19, 20] for a PM WDM signal using RP1. This study led to an accurate model with a closed-form expression for the nonlinear noise. For a single-channel PM non-DM link, a Gaussian model was proposed in [21] based on the split-step Fourier method (SSFM), which yielded a closed-form expression for the nonlinear noise. Numerical and experimental results [22, 23] showed a good agreement with the analytical model introduced in [15, 19, 20].

In our earlier work [21] for a non-DM fiber-optical channel with EDC, we showed that the derived analytical model has a close performance agreement with the numerical simulations. In this paper, we extend this analytical method for the non-DM fiber-optical channel, to include digital backpropagation (DBP) as a pre-compensation technique. In fact, the numerical simulations show almost the same performance for DBP used as a pre- or post compensator. Therefore, we consider a pre-compensation scheme based on DBP for simplicity of the analysis. As in [21], we take into account the cross effect of the signals in both polarizations. In contrast to previous works [15, 19, 24], we include the inline interaction between the transmitted signal and the amplified spontaneous emission (ASE) noise in different spans due to the Kerr effect. Then, we use a first-order approximation for the Taylor expansion of the nonlinear noise variance with respect to ASE noise variance. This helps us compute the variance of the nonlinear noise as a function of the transmit power, ASE noise variance, and channel parameters. The results show a quadratic growth of the nonlinear noise variance with input power for the system with DBP. The symbol error rate (SER) of a PM quadrature phase shift keying (QPSK) and PM 16-ary quadrature amplitude modulation (16-QAM) system is computed using this approximation and also by the numerical SSFM. The performance comparison shows a close agreement between the first-order approximation and numerical results for low and moderate transmit powers but they deviate for high transmit powers.

2. Channel Model

The propagation of light in an optical fiber can be described by Manakov model with loss included as [25, ch. 6]

$$j\frac{\partial \mathbf{U}(t,z)}{\partial z} - \frac{\beta_2}{2}\frac{\partial^2 \mathbf{U}(t,z)}{\partial t^2} + \gamma(\mathbf{U}(t,z)\mathbf{U}(t,z)^{\dagger})\mathbf{U}(t,z) + j\frac{\alpha}{2}\mathbf{U}(t,z) = \mathbf{0}, \tag{1}$$

where $\mathbf{U}$ is the PM electric field with complex components $(U_{\mathrm{x}}, U_{\mathrm{y}})$, γ is the fiber nonlinear coefficient, α is the attenuation coefficient, β_2 is the group velocity dispersion, $\dagger$ denotes Hermitian conjugation, t is the time coordinate in a co-moving reference frame and z is the propagation distance. A fiber-optical link with N spans of length L is considered according to Fig. 1. Each span consists of a standard single-mode fiber (SMF) followed by an erbium-doped fiber amplifier (EDFA).

#191784 - $15.00 USD Received 5 Jun 2013; revised 6 Sep 2013; accepted 20 Sep 2013; published 28 Oct 2013

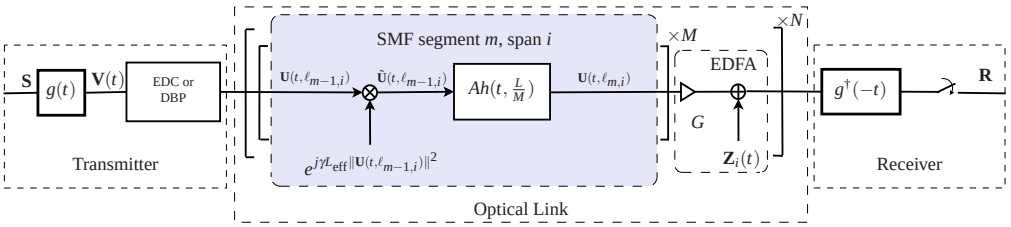

Fig. 1. A baseband continuous-time model based on the SSFM for a fiber-optical link with N spans of SMF fiber ($i = 1,\ldots,N$), each consisting of M segments ($m = 1,\ldots,M$), and electronic linear (EDC) and nonlinear (DBP) pre-compensation.

2.1. *Continuous-Time Channel Model*

One may exploit the SSFM [25, Eq. (2.4.10)] to model each SMF span by a concatenation of M segments with linear and nonlinear effects as shown in Fig. 1. The length of each segment, L/M, should be chosen small enough so that the linear and nonlinear effects can be modeled independently. The nonlinear effect of segment m of span i is given by $\tilde{\mathbf{U}}(t,\ell_{m-1,i}) = \mathbf{U}(t,\ell_{m-1,i})\exp(j\gamma L_{\text{eff}}\|\mathbf{U}(t,\ell_{m-1,i})\|^2)$, for $m = 1,\ldots,M$, where $L_{\text{eff}} = [1-\exp(-\alpha L/M)]/\alpha$, $\ell_{m,i} = m(L/M)+(i-1)L$, and $\ell_{0,i} = (i-1)L$. The linear propagation is described in the time domain by $\mathbf{U}(t,z) = \exp(-\alpha z/2)\mathbf{U}(t,0) * h(t,z)$, where $*$ denotes convolution, which is performed independently over elements of the vectors, and $h(t,z) = \exp[jt^2/(2\beta_2 z)]/\sqrt{j2\pi\beta_2 z}$ is the dispersive impulse response. As shown in Fig. 1, the linear effect in each segment is described by $\mathbf{U}(t,\ell_{m,i}) = A\tilde{\mathbf{U}}(t,\ell_{m-1,i}) * h(t,L/M)$, where $A \triangleq \exp[-\alpha L/(2M)]$ is the signal attenuation for each segment. The symbols $\mathbf{S}[n] = (S_{\text{x}}[n], S_{\text{y}}[n])$, e.g., PM QPSK, are transmitted every T seconds with a pulse shaping filter $g(t)$ and received as the distorted symbol sequence $\mathbf{R}$. It is assumed that $\mathbb{E}\{|S_{\text{x}}[n]|^2\} = \mathbb{E}\{|S_{\text{y}}[n]|^2\} = PT$, where P is the average transmitted power in one polarization. We assume that each EDFA compensates for the attenuation in each fiber span and adds a circular white complex Gaussian ASE noise vector, $\mathbf{Z}_i(t) = (Z_{\text{x}_i}(t), Z_{\text{y}_i}(t))$, in each span with variance (over the signal bandwidth) $\sigma^2 = GF_n h\nu_{\text{opt}}/(2T)$ in each polarization [26, Eq. (8.1.15)], where $G = \exp(\alpha L)$ is the required gain to compensate for the attenuation in a span, $F_n = 2n_{\text{sp}}(1-G^{-1})$ is the noise figure, in which n_{sp} is ASE noise factor, and $h\nu_{\text{opt}}$ is the photon energy. The optical bandwidth of the EDFAs is assumed to be equal to the signal bandwidth.

The fiber-optical link is analyzed for both EDC and DBP as shown in Fig. 1. In order to apply an analytical approach, we consider sinc-shaped pulses $g(t)$. However, the numerical results show that the proposed model is not very dependent on the exact pulse shape, e.g., root raised cosine and Gaussian pulses can be used as well. A filter matched to the pulse shape and a Nyquist sampler is assumed at the receiver (with perfect carrier and timing synchronization). Finally, we define the nonlinear phase shifts for the signal $\phi_{\text{s}} \triangleq \gamma\alpha^{-1}P$, and noise $\phi_{\text{n}} \triangleq \gamma\alpha^{-1}\sigma^2$, and the dispersion length [25, p. 55] $L_{\text{D}} = T^2/|\beta_2|$.

2.2. *Discrete-Time Channel Model*

In this section, we introduce a discrete-time model for segment m of span i of the continuous-time model, depicted in Fig. 1 with both linear and nonlinear pre-compensation. In the continuous-time model considering $g(t) = \text{sinc}(t/T)/\sqrt{T}$ as a pulse shape, where $\text{sinc}(x) = (\sin\,\pi x)/(\pi x)$, the transmitted signal is band-limited to $[-1/2T, 1/2T]$. Hereafter, we assume a pseudolinear fiber-optical data transmission, and therefore we neglect the spectral broadening due to the nonlinear effects, i.e., the bandwidth of $U_{\text{x}}(t)e^{j\gamma L_{\text{eff}}\|\mathbf{U}(t)\|^2}$ is assumed to be limited to $1/T$. This assumption helps us obtain the discrete-time model depicted in Fig. 2(b) to fulfill the

#191784 - $15.00 USD Received 5 Jun 2013; revised 6 Sep 2013; accepted 20 Sep 2013; published 28 Oct 2013

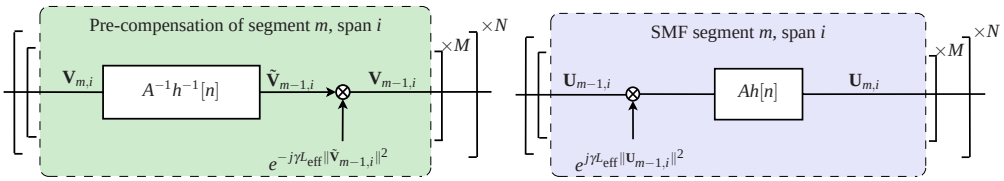

Fig. 2. (a) Nonlinear pre-compensation based on the DBP [27] ($h^{-1}[n]$ is the inverse of the filter $h[n]$). (b) A baseband discrete-time model for the SMF.

Nyquist criterion for sampling the continuous-time signals with a sampling rate of $1/T$. The discrete band-limited chromatic dispersion filter is given by $h[n] = h(t, L/M) * \text{sinc}(t/T)\big|_{t=nT}$ and h^{-1} is its inverse, i.e., $h[n] * h^{-1}[n] = \delta[n]$, where $\delta[n]$ is the Kronecker's delta.

3. Statistics of the Propagated Signal Using the Split-Step Fourier Method

In this section, we first review our previous results on the signal statistics for a single channel fiber-optical link with EDC [21]. Then, we use the same framework as in [21] to study the signal statistics with DBP.

The distribution of the signal for a PM single-channel fiber-optical link is derived in [21] with large accumulated dispersion and without inline chromatic dispersion compensation. According to this model, the fiber-optical link depicted in Fig. 1 can be modeled as a linear channel with an additive Gaussian noise described by

$$\mathbf{R} = \zeta \mathbf{S} + \mathbf{W}, \tag{2}$$

where ζ is a complex constant, $\mathbf{S}$ is the sequence of symbols $\mathbf{S}[n]$ introduced in Section 2.1, and $\mathbf{W}$ represents the PM complex zero-mean circularly symmetric AWGN.

3.1. Signal Statistics with EDC

The squared amplitude of the channel complex scaling constant ζ for the EDC case is given by

$$|\zeta_{\text{EDC}}|^2 \approx 1 - 3N^{1+\varepsilon}\phi_{\text{s}}^2 \tanh(\tfrac{\alpha}{4}L_{\text{D}}). \tag{3}$$

Experimental investigations [23, 28] on the accumulation of nonlinear noise versus the number of spans, N, revealed that the nonlinear noises from different spans sum up partially coherently rather than entirely incoherently as was approximated in [21]. Therefore, as introduced in [15, Eq. (23)], we considered $N^{1+\varepsilon}$ rather than N to account for this behavior of the nonlinear noise, where

$$\varepsilon = \tfrac{3}{10}\log\left(1 + \frac{6}{\alpha L \,\text{asinh}\left(\frac{\pi^2}{2\alpha L_{\text{D}}}\right)}\right). \tag{4}$$

The system signal-to-noise ratio (SNR) is given by $|\zeta_{\text{EDC}}|^2 P/(N\sigma^2 + \sigma_{\text{NL}}^2)$, where

$$\sigma_{\text{NL}}^2 = (1 - |\zeta_{\text{EDC}}|^2)P \approx 3N^{1+\varepsilon}\gamma^2\alpha^{-2}\tanh(\tfrac{\alpha}{4}L_{\text{D}})P^3. \tag{5}$$

#191784 - $15.00 USD Received 5 Jun 2013; revised 6 Sep 2013; accepted 20 Sep 2013; published 28 Oct 2013

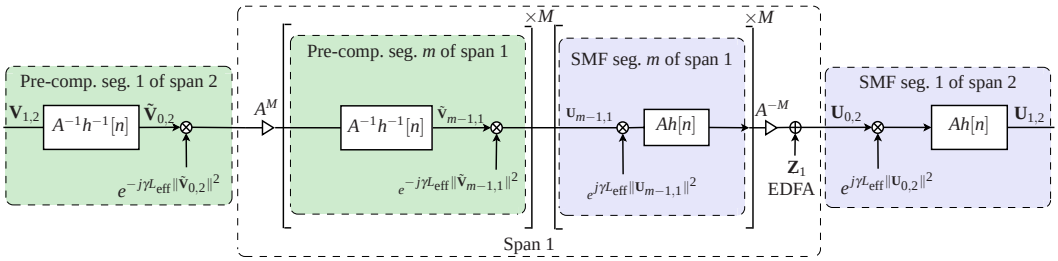

Fig. 3. The discrete-time model of segment 1 from span 2 and the first span together with their corresponding pre-compensation units. The gain of the EDFA unit is assumed to be canceled out by the compensation unit. The channel deterministic impairments are fully compensated for the first span because the first amplifier is assumed to be added at the beginning of the second span. All the impairments for the first span are deterministic and there is no noise interaction involved in the signal propagation in this span.

As showed in [21], the contribution of signal–noise interaction to the variance of the nonlinear noise can be neglected compared to the contribution of the signal–signal interaction and the amplifier noise for a system with EDC. Moreover, since the power loss in the fiber-optical link is compensated by inline amplifiers, the attenuation caused by the complex scaling constant with $|\zeta|^2 < 1$, is coming from the fact that the nonlinear effect converts a part of the transmitted power to the nonlinear noise. The comparison in Section 4 shows a good agreement between our proposed model using Eqs. (3) and (5), the model introduced in [15, Eqs. (7), (13), and (23)] and numerical simulations.

3.2. Signal Statistics with DBP

In this section, we use an analogous analytical method as [21] to derive the variance of the nonlinear noise for a system with DBP as pre-compensation technique. As shown in Appendix, the complex constant for segment m of span i for the fiber-optical link shown in Fig. 3 is

$$|\zeta_{\text{DBP}_{m,i}}|^2 \approx 1 - 6(i-1)A^{4(m-1)}\alpha^2 L_{\text{eff}}^2 \phi_{\text{s}} \phi_{\text{n}}. \tag{6}$$

The complex constant ζ_{DBP} for the fiber-optical link with N spans can be derived as

$$|\zeta_{\text{DBP}}|^2 = \prod_{i=1}^{N}\prod_{m=1}^{M} |\zeta_{\text{DBP}_{m,i}}|^2 \approx 1 - 6\alpha^2 L_{\text{eff}}^2 \phi_{\text{s}} \phi_{\text{n}} \sum_{i=1}^{N}\sum_{m=1}^{M} (i-1)A^{4(m-1)}. \tag{7}$$

The SER is computed by $2Q(\sqrt{\text{SNR}}) - Q^2(\sqrt{\text{SNR}})$ [30, Eq. 4.3-15] and $3Q(\sqrt{\text{SNR}}) - 9Q^2(\sqrt{\text{SNR}})/4$ [30, Eq. 4.3-30] for PM QPSK and PM 16-QAM signals, respectively, where $\text{SNR} = |\zeta_{\text{DBP}}|^2 P/(N\sigma^2 + (1-|\zeta_{\text{DBP}}|^2)P)$ and $Q(\cdot)$ is the Gaussian Q-function [30, p. 41]. By using an empirical approach, we found that Eq. (7) with a segment length around $L_{\text{D}}/2$ provides an approximation for the SERs of the system with DBP, which is tight for low and moderate powers (as shown in Fig. 4(b)). Intuitively, to return the non-Gaussian distribution caused by the nonlinear effect in the SMF fiber to the Gaussian distribution described in Section 2.2 for the SSFM, a large enough segment length is needed to have enough chromatic dispersion for fulfilling the central limit theorem condition [21]. On the other hand, to obtain enough accuracy for the SSFM, the segment length needs to be kept short. In brief, the SER is intimately related to the proper choice of the segment length. To obtain a good trade-off between the accuracy of the Gaussian assumption and the SSFM method, we consider $M = \lceil 2L/L_{\text{D}} \rceil$, where $\lceil x \rceil$ is the

#191784 - $15.00 USD Received 5 Jun 2013; revised 6 Sep 2013; accepted 20 Sep 2013; published 28 Oct 2013

the smallest integer value that is not less than x. Thus, we have

$$|\zeta_{\mathrm{DBP}}|^2 \approx 1 - 3N^{1+\varepsilon}(N-1)\phi_{\mathrm{s}}\phi_{\mathrm{n}}\tanh(\tfrac{\alpha}{4}L_{\mathrm{D}}). \tag{8}$$

In an analogous way as in Section 3.1, we assume the nonlinear noise to sum up partially coherently and therefore modified its linear growth to $N^{1+\varepsilon}$ to account for this behavior. For a sinc pulse shape, $\mathbf{S} = \mathbf{V}_{M,N}$, $\mathbf{R} = \mathbf{U}_{M,N}$, and the all-pass matched filter, depicted in Fig. 1, does not change the distribution and the variance of the AWGN noise $\mathbf{W}$. Therefore, the variance of $\mathbf{W} = (W_{\mathrm{x}}, W_{\mathrm{y}})$ is obtained as

$$\mathrm{Var}\{W_{\mathrm{x}}\} = \mathrm{Var}\{W_{\mathrm{y}}\} \approx \left(1 - |\zeta|^2\right) P + N\sigma^2 = 3N^{1+\varepsilon}(N-1)\gamma^2\alpha^{-2}\sigma^2\tanh(\tfrac{\alpha}{4}L_{\mathrm{D}})P^2 + N\sigma^2, \tag{9}$$

This result brings us to the conclusion that the fiber-optical link with N spans and its nonlinear pre-compensator based on DBP can be modeled as a linear channel with the complex constant attenuation ζ_{DBP} and the AWGN $\mathbf{W}$, introduced in Eqs. (8) and (9), respectively.

4. Numerical Simulations

In this section, we evaluate the accuracy of the derived first-order approximation for two fiber-optical links with PM QPSK and PM 16-QAM signals at 32 and 42.7 Gbauds. The analytical SERs are also evaluated using Eqs. (3)–(5) for EDC and the first-order approximation by Eqs. (8)–(9) for DBP. The SSFM [25, Eq. (2.4.10)] is used to simulate a fiber-optical channel based on the Manakov equation with an adaptive segment length [31] of $\Delta_i = (\kappa L_{\mathrm{N}} L_{\mathrm{D}}^2)^{1/3}$, where i is the segment index, $\kappa = 10^{-4}$ and $L_{\mathrm{N}} = 1/(\gamma P_{i-1})$ is the nonlinear length of segment $i-1$ [25, p. 55] with the input power P_{i-1}. In the simulations, a root raised cosine pulse [30, p. 675] was used with an excess bandwidth of 0.17 and a truncation length of 16 symbols as well as input sequences consisting of 8192 discrete-time symbols to capture the channel memory (dispersion crosstalk). For each SER, we repeatedly transmit and receive sequences of 8192 symbols until we have 1000 symbol errors. The input bits to the PM QPSK and PM 16-QAM modulators are generated as independent, uniform random binary digits. The following channel parameters are used for the numerical simulations: the dispersion coefficient $D = 17$ ps/(nm km), the nonlinear coefficient $\gamma = 1.4\ \mathrm{W}^{-1}\mathrm{km}^{-1}$, the optical wavelength $\lambda = 1.55\ \mu$m, the attenuation coefficient $\alpha = 0.2$ dB/km, and the EDFA noise figure $F_{\mathrm{n}} = 5$ dB.

The SERs versus transmitted power per polarization P of two fiber-optical links with EDC for PM QPSK are shown in Fig. 4(a). For the numerical simulation, we use the links consisting of 90 spans of length 80 km at 32 Gbaud and 30 spans of length 120 km at 42.7 Gbaud. The pulse shaping excess bandwidth and the symbol rates for the numerical simulations are chosen to obtain two signal bandwidths of 37.5 and 50 GHz. It is worth mentioning that the first-order approximation derived in this paper is also applicable for WDM systems where intra-channel effects are dominant, for example a WDM system with few channels and large frequency spacing between the channels. The SERs of these two systems with EDC have also been evaluated analytically using Eqs. (3), (5), and [15, Eqs. (7), (13), and (23)]. As seen, the analytical models show a good agreement with the numerical simulations for low and moderate transmit powers, almost up to the optimal power, the so-called nonlinear threshold. For high transmit powers, the pseudolinear assumption (see Section 2.2) is not valid anymore, which causes discrepancy between the simulations and analytical approach.

The SERs of a fiber-optical link with DBP as pre-compensation technique are plotted in Fig. 4(b) for two different system configurations: 70 spans of length 120 km with a QPSK signal and 100 spans of length 80 km with a 16-QAM signal, both at 32 Gbaud. We observed a similar behavior as with 32 Gbaud for higher baud rates, e.g., 42.7 Gbaud. As seen, the first-

#191784 - $15.00 USD Received 5 Jun 2013; revised 6 Sep 2013; accepted 20 Sep 2013; published 28 Oct 2013

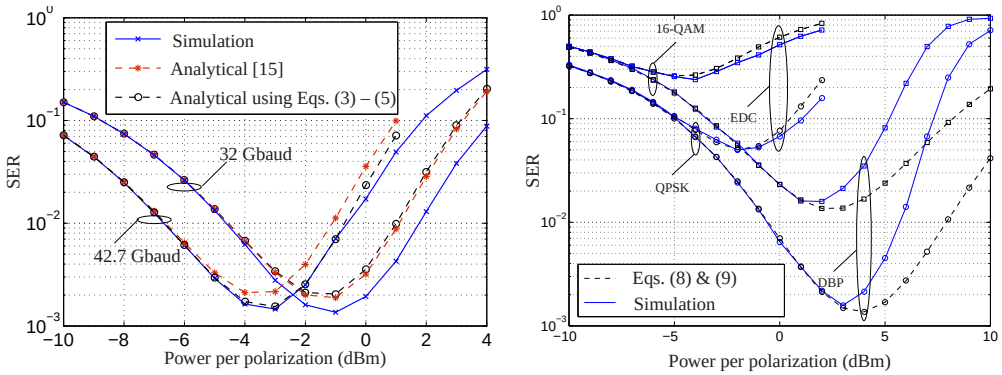

(a) (b)

Fig. 4. (a) The SERs of two fiber-optical links with EDC and PM QPSK versus transmitted power per polarization P, consisting of 90 spans of length 80 km at 42.7 Gbaud and 30 spans of length 120 km at 32 Gbaud. The analytical results using the introduced model in Eqs. (3) – (5) as well as the model in [15, Eqs. (7), (13), and (23)]. (b) The SERs of two systems consisting of 70 spans of length 120 km with a QPSK signal and 100 spans of length 80 km with a 16-QAM signal, both at 32 Gbaud.

order approximation of the system SERs shows a good agreement with the simulation results for EDC. The system SERs with DBP using the first-order approximation in Fig. 4(b) show a good agreement for low and moderate transmit powers, while for high transmit powers the Gaussian model underestimates the degradation caused by nonlinear effects. In fact, for high transmit powers, the fundamental requirement of the Gaussian noise model, operating in the pseudolinear regime, i.e., when the dispersive length is much shorter than the nonlinear length, and also shorter than the amplifier distance, is not fulfilled.

5. Discussions and Conclusions

5.1. Gaussian Assumption

The numerical simulation of the NLSE is usually performed using the SSFM with a very small segment length to ensure that linear dispersive and nonlinear effects can be modeled independently. As shown analytically in [21], for a link with large enough accumulated chromatic dispersion, the distribution of the electric field will turn to Gaussian for signals with large enough bandwidth (dispersion) in the absence of nonlinear effects. Moreover, since the nonlinear effect will change the distribution of the signal to a non-Gaussian distribution in each segment of the SSFM, a large enough segment length is required to bring the signal distribution back to Gaussian [9, 21].

5.1.1. Non-DM link with EDC

The analytical model introduced in [21] was obtained using a segment length between $0.5L_D$ and L_D (or equivalently $\lceil 2L/L_D \rceil$ segments per span). The SER results show a good agreement with the numerical results computed by the SSFM. If one chooses $\varepsilon = 0$, our simulations show that SER is underestimated for the EDC case just as for the DBP case because Gaussian assumption loses its accuracy. However, when ε as given by Eq. (4) is used, the SER is overestimated as shown in Fig. 4(a). This is due to partially coherent accumulation of noises from different spans.

#191784 - $15.00 USD Received 5 Jun 2013; revised 6 Sep 2013; accepted 20 Sep 2013; published 28 Oct 2013

Table 1. The variance of the additive Gaussian noise W_x and W_y introduced in Eq. (2) with EDC and DBP consisting of the linear (ASE) and nonlinear noise-like interference.

EDC	$a_{\mathrm{NL}}P^3 + N\sigma^2$
DBP	$a_{\mathrm{NL}}(N-1)\sigma^2P^2 + N\sigma^2$
Scale factor	$a_{\mathrm{NL}} = 3N^{1+\varepsilon}\gamma^2\alpha^{-2}\tanh(\frac{\alpha}{4}L_{\mathrm{D}})$

5.1.2. Non-DM link with DBP

Since the segment length required for the SSFM simulation of the channel is much less than $0.5L_D$, a similar segment length is needed for DBP to get the best (minimum) SER [29]. On the other hand, a large segment length is needed to have enough chromatic dispersion for fulfilling the central limit theorem condition [21]. To obtain a good trade-off between the accuracy of the Gaussian assumption and the SSFM, we considered a segment length of $0.5L_{\mathrm{D}}$ for the first-order approximation. As discussed in Section 4, the SERs computed by the first-order approximation have a good agreement with the numerical results based on the SSFM for low and moderate transmit powers, while they can be only used as a lower bound on the SER at large transmit powers.

5.2. Nonlinear Threshold

As shown by numerical simulations, the first-order approximation is reasonably tight for different symbol rates and it can be used to compute approximately the optimum transmit power in terms of minimizing SER. Therefore, at the optimum power, i.e., nonlinear threshold, the variance of the nonlinear noise is equal to the variance of the accumulated ASE noises, while for a system with EDC, the ASE noise variance is known to be twice the nonlinear noise variance [33]. Moreover, the first-order approximation results show the quadratic growth of the nonlinear noise with transmitted power, which is a limit for the performance of a system with DBP.

5.3. Growth of Nonlinear Noise with Transmit Power

The numerical results show that the discrete-time additive Gaussian noise channel model described by Eq. (2) can be used as an accurate model for a non-DM fiber-optical link with both linear (EDC) and nonlinear (DBP) pre-compensation for low and moderate transmit powers. As shown in Table 1, the signal–signal nonlinear interference caused by the Kerr effect can be removed to mitigate the cubic growth of the nonlinear noise variance of a system with EDC to a quadratic growth with DBP. This behavior is intuitively predictable. In fact, within the regular perturbation assumption [6,15,17,18], the nonlinear noise comes from the integration of electric field terms $\mathbf{U}\mathbf{U}^{\dagger}\mathbf{U}$ whose variance scales as P^3. In the presence of ASE noise, the nonlinear noise of the RP1 comes from terms $\mathbf{U}\mathbf{U}^{\dagger}(\mathbf{U}+\mathbf{Z}) = \mathbf{U}\mathbf{U}^{\dagger}\mathbf{U} + \mathbf{U}\mathbf{U}^{\dagger}\mathbf{Z}$. When the solely signal-dependent nonlinear noise term $\mathbf{U}\mathbf{U}^{\dagger}\mathbf{U}$ is perfectly compensated by DBP, then the leftover nonlinear noise is in order of $\mathbf{U}\mathbf{U}^{\dagger}\mathbf{Z}$, whose variance clearly scales as P^2.

Acknowledgments

The authors would like to thank the Swedish Foundation for Strategic Research, SSF, and VINNOVA for their funding of this research under grants RE07-0026 and 2010-01238, respectively.

The calculations were performed in part on resources provided by the Swedish National Infrastructure for Computing (SNIC) at C3SE.

Appendix

A. Derivation of the nonlinear noise variance for a system with DBP

We use an analogous analytical method as [21] to derive the variance of the nonlinear noise for a system with DBP.

A.1. Span 1

As illustrated in Fig. 3, the channel impairments can be fully compensated for the first span, because all the impairments for the first span are deterministic and there is no noise interaction involved in the signal propagation in this span. We would like to point out that this is however not true for post-compensation, i.e., DBP at the receiver. However, according to the numerical results (not provided in this paper), having DBP at the receiver gives rise to a negligible performance loss compared with DBP at transmitter.

A.2. First Segment of Span 2

As seen in Fig. 3, the first ASE noise vector, $\mathbf{Z}_1 = (Z_{\mathrm{x}_1}, Z_{\mathrm{y}_1})$ is added at the end of the first span $i = 1$. The discrete-time models introduced for the SMF fiber and the nonlinear pre-compensator can be used to derive the equivalent discrete-time model for the first segment of span 2, $m = 1, i = 2$, as shown in Fig. 3. The signal $\mathbf{U}_{1,2}$ at the output of the first segment of span 2 can be written as

$$\mathbf{U}_{1,2} = A\left(\mathbf{U}_{0,2} e^{j\gamma L_{\mathrm{eff}} \|\mathbf{U}_{0,2}\|^2}\right) * h = A\left(\left(\tilde{\mathbf{V}}_{0,2} + \mathbf{Z}_1'\right) e^{j\gamma L_{\mathrm{eff}} \left(\|\tilde{\mathbf{V}}_{0,2} + \mathbf{Z}_1'\|^2 - \|\tilde{\mathbf{V}}_{0,2}\|^2\right)}\right) * h, \tag{10}$$

where $U_{1,2} = (U_{\mathrm{x}_{1,2}}, U_{\mathrm{y}_{1,2}})$, $\mathbf{Z}_1' = (Z_{\mathrm{x}_1}', Z_{\mathrm{y}_1}') = \mathbf{Z}_1 e^{j\gamma L_{\mathrm{eff}} \|\tilde{\mathbf{V}}_{0,2}\|^2}$ is a zero-mean complex Gaussian random vector with the same covariance matrix as $\mathbf{Z}_1$, and $\tilde{\mathbf{V}}_{0,2} = A^{-1}\mathbf{V}_{1,2} * h^{-1}$. We notice that the DBP pre-compensator contributes the second term into the exponent of the exponential function of Eq. (10). As the analysis shows shortly, this term mitigates the nonlinear effect considerably. Hence, $\mathbf{U}_{0,2} = (\tilde{\mathbf{V}}_{0,2} + \mathbf{Z}_1')e^{-j\gamma L_{\mathrm{eff}} \|\tilde{\mathbf{V}}_{0,2}\|^2}$. By some algebraic manipulations, one can write $\mathbf{U}_{1,2} = \zeta_{\mathrm{DBP}_{1,2}} \mathbf{V}_{1,2} + \mathbf{W}_{1,2}$, where

$$\mathbf{W}_{1,2} = A\Big((\tilde{\mathbf{V}}_{0,2} + \mathbf{Z}_1')e^{j\gamma L_{\mathrm{eff}} \left(\|\tilde{\mathbf{V}}_{0,2} + \mathbf{Z}_1'\|^2 - \|\tilde{\mathbf{V}}_{0,2}\|^2\right)} - \zeta_{\mathrm{DBP}_{1,2}} \tilde{\mathbf{V}}_{0,2}\Big) * h. \tag{11}$$

Here, the complex constant $\zeta_{\mathrm{DBP}_{1,2}}$ is computed such that $\mathbb{E}\{\mathbf{W}_{1,2}\} = \mathbf{0}$. Thus,

$$\mathbb{E}\{\mathbf{W}_{1,2}\} = A\mathbb{E}\Big\{(\tilde{\mathbf{V}}_{0,2} + \mathbf{Z}_1')e^{j\gamma L_{\mathrm{eff}} \left(\|\tilde{\mathbf{V}}_{0,2} + \mathbf{Z}_1'\|^2 - \|\tilde{\mathbf{V}}_{0,2}\|^2\right)} - \zeta_{\mathrm{DBP}_{1,2}} \tilde{\mathbf{V}}_{0,2}\Big\} * h = \mathbf{0}. \tag{12}$$

For a non-DM fiber-optical link, the chromatic dispersion will turn the distribution of the optical field into a zero-mean Gaussian process [21]. Thus, we have $|\mathbb{E}\{\tilde{V}_{\mathrm{x}_{0,2}}\}|^2 = |\mathbb{E}\{\tilde{V}_{\mathrm{y}_{0,2}}\}|^2 \approx 0$ and with some algebraic manipulations we obtain $\zeta_{\mathrm{DBP}_{1,2}}^{-1} \approx (1 + \alpha^2 L_{\mathrm{eff}}^2 \phi_{\mathrm{s}} \phi_{\mathrm{n}} - j\alpha L_{\mathrm{eff}} \phi_{\mathrm{n}})^3$. Thus, for low transmit power P, one may perform a Taylor expansion and ignore the terms consisting of ϕ_{s} with order 3 and higher and ϕ_{n} with order 2 and higher to get

$$|\zeta_{\mathrm{DBP}_{1,2}}|^2 \approx 1 - 6\alpha^2 L_{\mathrm{eff}}^2 \phi_{\mathrm{n}} \phi_{\mathrm{s}}. \tag{13}$$

The variance of the additive linear (ASE) and nonlinear noise is $\mathrm{Var}\{W_{\mathrm{DBP}_{1,2}}\} = (1 -$

#191784 - $15.00 USD Received 5 Jun 2013; revised 6 Sep 2013; accepted 20 Sep 2013; published 28 Oct 2013

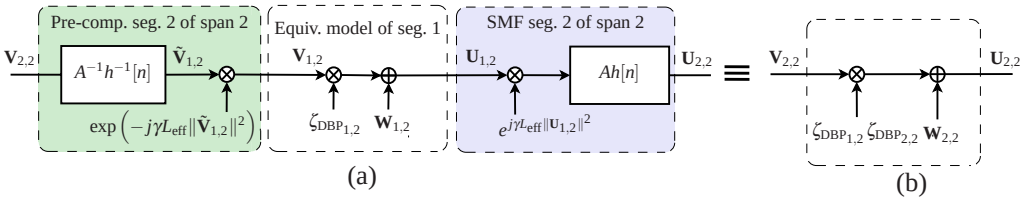

Fig. 5. (a) The discrete-time model of segment 2 and its pre-compensation unit from span 2 together with the simplified model of segment 1. (b) The simplified model for segments 1 and 2 and their corresponding pre-compensation units.

$|\zeta_{\text{DBP}_{1,2}}|^2)P+\sigma^2 \approx 6\alpha^3\gamma^{-1}L_{\text{eff}}^2\phi_{\text{s}}^2\phi_{\text{n}}+\sigma^2$. This result brings us to the conclusion that segment 1 and its nonlinear pre-compensator can be modeled as a linear channel with the additive Gaussian noise $\mathbf{W}_{1,2}$ and complex constant attenuation $\zeta_{\text{DBP}_{1,2}}$ as shown in Fig. 5.

A.3. Second Segment of Span 2

Since we postulate that the additive Gaussian noise and the channel complex scaling are signal independent, one may follow the same approach as used for segment 1 to find an equivalent model for segment 2. As seen in Fig. 5, using the discrete-time model introduced for the SMF fiber and the nonlinear pre-compensator for segment 2 of span 2, one can write

$$\mathbf{U}_{2,2}=A\left(\mathbf{U}_{1,2}e^{j\gamma L_{\text{eff}}\|\mathbf{U}_{1,2}\|^2}\right)*h=A\Big((\zeta_{\text{DBP}_{1,2}}\tilde{\mathbf{V}}_{1,2}+\mathbf{W}'_{1,2})e^{j\gamma L_{\text{eff}}\left(\|\zeta_{\text{DBP}_{1,2}}\tilde{\mathbf{V}}_{1,2}+\mathbf{W}'_{1,2}\|^2-\|\tilde{\mathbf{V}}_{1,2}\|^2\right)}\Big)*h, \quad (14)$$

where $\mathbf{U}_{2,2}=(U_{\text{x}_{2,2}},U_{\text{y}_{2,2}})$ and $\mathbf{W}'_{1,2}=\mathbf{W}_{1,2}e^{j\gamma L_{\text{eff}}\|\tilde{\mathbf{V}}_{1,2}\|^2}$. By some algebraic manipulations, one can write $\mathbf{U}_{2,2}=\zeta_{\text{DBP}_{2,2}}\zeta_{\text{DBP}_{1,2}}\mathbf{V}_{2,2}+\mathbf{W}_{2,2}$, where

$$\mathbf{W}_{2,2}=A\Big((\zeta_{\text{DBP}_{1,2}}\tilde{\mathbf{V}}_{1,2}+\mathbf{W}'_{1,2})e^{j\gamma L_{\text{eff}}\left(\|\zeta_{\text{DBP}_{1,2}}\tilde{\mathbf{V}}_{1,2}+\mathbf{W}'_{1,2}\|^2-\|\tilde{\mathbf{V}}_{1,2}\|^2\right)}-\zeta_{\text{DBP}_{2,2}}\zeta_{\text{DBP}_{1,2}}\tilde{\mathbf{V}}_{1,2}\Big)*h. \quad (15)$$

Here, $\zeta_{\text{DBP}_{2,2}}$ is computed such that $\mathbb{E}\{\mathbf{W}_{2,2}\}=\mathbf{0}$. Using $|\mathbb{E}\{\tilde{V}_{\text{x}_{1,2}}\}|^2=|\mathbb{E}\{\tilde{V}_{\text{y}_{1,2}}\}|^2\approx 0$ for a non-DM channel and some algebraic manipulations, we obtain $\zeta_{\text{DBP}_{2,2}}\approx(1+\alpha^2L_{\text{eff}}^2A^2|\zeta_{\text{DBP}_{1,2}}|^2\phi_{\text{s}}\tilde{\phi}_{\text{n}}-j\alpha L_{\text{eff}}\tilde{\phi}_{\text{n}})^{-3}$, where $\tilde{\phi}_{\text{n}}=A^2\phi_{\text{n}}+A^2(1-|\zeta_{\text{DBP}_{0,2}}|^2)\phi_{\text{s}}$. Similarly, one may perform a Taylor expansion with respect to ϕ_{s} and ϕ_{n} and use Eq. (13) and also ignore the terms consisting of ϕ_{s} with order greater or equal to 3 and ϕ_{n} with order 2 and higher to get

$$|\zeta_{\text{DBP}_{2,2}}|^2\approx 1-6A^4\alpha^2L_{\text{eff}}^2\phi_{\text{s}}\phi_{\text{n}}. \quad (16)$$

A.4. General segment and full link

One may follow an analogous approach to derive the complex constant for segment m of span i from the fiber-optical link shown in Fig. 3 as

$$|\zeta_{\text{DBP}_{m,i}}|^2\approx 1-6(i-1)A^{4(m-1)}\alpha^2L_{\text{eff}}^2\phi_{\text{s}}\phi_{\text{n}}, \quad (17)$$

and the complex constant for the full link will be $|\zeta_{\text{DBP}}|^2=\prod_{i=1}^{N}\prod_{m=1}^{M}|\zeta_{\text{DBP}_{m,i}}|^2$.

#191784 - $15.00 USD Received 5 Jun 2013; revised 6 Sep 2013; accepted 20 Sep 2013; published 28 Oct 2013